PROCEEDINGS B

royalsocietypublishing.org/journal/rspb

Research

Cite this article: Tomalka A, Röhrle O, Han J-C, Pham T, Taberner AJ, Siebert T. 2019 Extensive eccentric contractions in intact cardiac trabeculae: revealing compelling differences in contractile behaviour compared to skeletal muscles. *Proc. R. Soc. B* **286**: 20190719.
http://dx.doi.org/10.1098/rspb.2019.0719

Received: 27 March 2019
Accepted: 7 May 2019

Subject Category:
Morphology and biomechanics

Subject Areas:
structural biology, biomechanics, physiology

Keywords:
heart muscle, titin–actin interactions, contractile properties, lengthening contractions, linear muscle behaviour, blebbistatin

Author for correspondence:
André Tomalka
e-mail: andre.tomalka@inspo.uni-stuttgart.de

Electronic supplementary material is available online at https://dx.doi.org/10.6084/m9.figshare.c.4502132.

THE ROYAL SOCIETY PUBLISHING

Extensive eccentric contractions in intact cardiac trabeculae: revealing compelling differences in contractile behaviour compared to skeletal muscles

André Tomalka[1], Oliver Röhrle[2,3], June-Chiew Han[4], Toan Pham[5], Andrew J. Taberner[4,6] and Tobias Siebert[1]

[1]Department of Motion and Exercise Science, and [2]Institute of Applied Mechanics (Civil Engineering), University of Stuttgart, Stuttgart, Germany
[3]Cluster of Excellence for Simulation Technology (SimTech), Stuttgart, Germany
[4]Auckland Bioengineering Institute, [5]Department of Physiology, and [6]Department of Engineering Science, The University of Auckland, Auckland, New Zealand

AT, 0000-0002-6957-5094; OR, 0000-0002-1934-6525; J-CH, 0000-0002-6396-7628; TP, 0000-0002-6323-9217; AJT, 0000-0002-0452-0308; TS, 0000-0003-4090-5480

Force enhancement (FE) is a phenomenon that is present in skeletal muscle. It is characterized by progressive forces upon active stretching—distinguished by a linear rise in force—and enhanced isometric force following stretching (residual FE (RFE)). In skeletal muscle, non-cross-bridge (XB) structures may account for this behaviour. So far, it is unknown whether differences between non-XB structures within the heart and skeletal muscle result in deviating contractile behaviour during and after eccentric contractions. Thus, we investigated the force response of intact cardiac trabeculae during and after isokinetic eccentric muscle contractions (10% of maximum shortening velocity) with extensive magnitudes of stretch (25% of optimum muscle length). The different contributions of XB and non-XB structures to the total muscle force were revealed by using an actomyosin inhibitor. For cardiac trabeculae, we found that the force–length dynamics during long stretch were similar to the total isometric force–length relation. This indicates that no (R)FE is present in cardiac muscle while stretching the muscle from 0.75 to 1.0 optimum muscle length. This finding is in contrast with the results obtained for skeletal muscle, in which (R)FE is present. Our data support the hypothesis that titin stiffness does not increase with activation in cardiac muscle.

1. Background

Force-producing mechanisms such as the cross-bridge (XB) and sliding filament theory have proved to be similar in cardiac and skeletal muscle tissues [1,2]. Yet, cardiac and skeletal muscle exhibit different contractile behaviour. These differences have been attributed to variations in the underlying non-cross-bridge (non-XB) structures. During systole, the heart muscle contracts concentrically only. The physiological working range is restricted to comparatively short sarcomere lengths (SL) that correspond in skeletal muscle to a working range associated with the ascending limb of the force–length relation (FLR) [2]. In cardiac muscle, the passive FLR is an exponential function originating at SLs of about 1.9 µm [3,4]. By contrast, skeletal muscles have relatively small passive forces, which start to rise at SLs around 2.5 µm (figure 1*b*) [6]. Skeletal muscles also exhibit a much larger working range [7], and operate as motor, spring or brake during locomotion [8,9]. Skeletal muscles generate higher active forces following stretch (residual force enhancement; RFE), if compared to the muscles' corresponding isometric force at constant length. This fact has been known for about 60 years [10] and has been confirmed on single sarcomeres [11], myofibrils [12], muscle fibres [13], single muscles [14] and

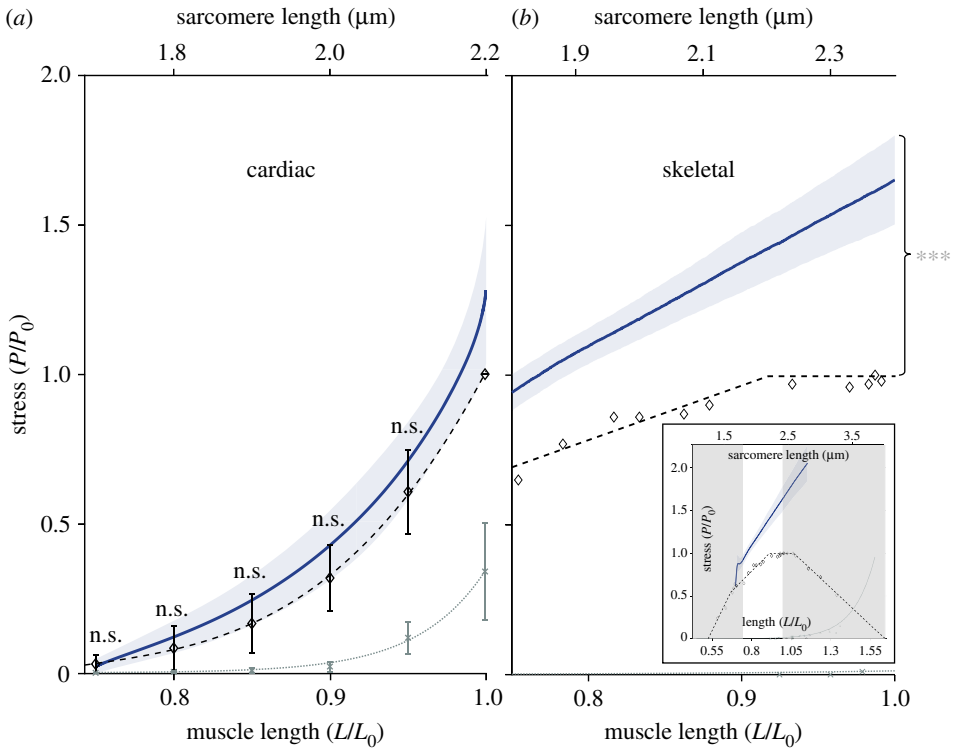

Figure 1. Isokinetic eccentric stretch contractions in (*a*) cardiac and (*b*) skeletal muscle. Blue solid lines indicate mean stress responses during an active isokinetic eccentric stretch. The shaded regions indicate the standard deviations. For comparison, the total isometric stress–length relation (black dashed line) and passive isometric stress–length relation (grey dotted line) are shown. Diamonds and crosses express the mean values of total and passive isometric muscle stresses, respectively. (*a*) Bars indicate corresponding standard deviations for lengths from 0.75 to 1.0 L/L_0, except for the mean values at 1.0 L_0 of total isometric stress–length dependency, as the stress is normalized to maximum isometric stress (P/P_0). The length is normalized to optimum muscle length (L/L_0, lower abscissa) or given as SL (µm) (upper abscissa), respectively. The mean values of cardiac muscles from the total isometric contraction (diamonds) were fitted to a third-order polynomial function (black dashed line), whereas those from the passive isometric contraction (crosses) were fitted using an exponential function (grey dotted line). A total of $n=11$ cardiac trabeculae were examined for all measurements. In all ramp experiments, the stretch velocity was 10% v_{max} yielding the blue solid line. The observed nonlinear stress response (blue solid line) in cardiac muscle was not statistically different (marked as 'n.s.') from the corresponding total isometric stress values at distinct lengths of 0.75 L_0, 0.8 L_0, 0.85 L_0, 0.9 L_0 and 0.95 L_0 (table 1). (*b*) For systematic comparison of contractile behaviour between cardiac and skeletal muscles during isokinetic eccentric stretching, measurements, obtained under similar experimental conditions as in the cardiac experiments for skinned skeletal fibres from EDL muscles are shown. In contrast with cardiac muscle, the characteristic linear spring behaviour (blue solid line) in skeletal muscle statistically exceeds ($p < 0.001$, as indicated by asterisks) the maximum total stresses over nearly the entire physiological working range (inset; unshaded region). Data reproduced from [5].

multi-joint movements [15]. Hereby, maximal RFE effects of up to 200% F_0 have been reported [16]. More recently, experiments on single muscle fibres extracted from the M. extensor digitorum longus (EDL) of the rat revealed that there also exists force enhancement (FE) during long eccentric stretches. This finding shows that skeletal muscle fibres behave like a linear spring over nearly the entire FLR (figure 1*b*, inset) [5]. To our knowledge, this phenomenon of linear behaviour during long eccentric muscle contractions has not been investigated using intact cardiac tissue preparations.

Despite the large number of experimental studies and a variety of attempts to explain FE in skeletal muscle, there is still a scientific debate regarding detailed molecular mechanisms and, therefore, no generally accepted model exists [17–20]. Titin [21], a huge filamentous protein, seems to play a crucial role in contributing to the enhanced force response during and following stretch contractions in skeletal muscle. Several model approaches [22–26] have been suggested, explaining FE in skeletal muscle—based on an adjustable titin spring—which were supported by experimental evidence for titin–actin interactions upon muscle activation [27–33]. There exists also contradictory studies that observed essentially no contribution of an adjustable titin spring [32,34] or even a reduction in titin–actin interactions with increased Ca^{2+} concentrations [30,31]. These investigations, however, have been done primarily on cardiac muscle tissue preparations. In the literature, one observes a lack of sharp differentiation between the distinct muscle tissue types. Hence, a transferability of results due to structural differences and methodological issues is doubtful. Further, the controversy might be due to a mixture/mismatch of experimental observations gathered from cardiac and skeletal tissue preparations. To date, there are only two studies investigating RFE in cardiac myofibrils [35,36]. However, they use permeabilized preparations obtained from homogenized ventricle muscle samples. Results revealed no RFE in permeabilized cardiac myofibrils.

Therefore, a structurally and physiologically based understanding of the influence of non-XB structures on cardiac muscle force is pending. The force response upon myocardial muscle stretching, which occurs during cardiac filling, is characterized by two distinct phenomena: by an instantaneous increase in twitch force, the so-called Frank–Starling mechanism [37] and by a several minute lasting slow increase in twitch, the so-called slow force response [38]. There is extensive evidence that titin

Table 1. Mean stress values ± s.d. normalized to P_0 of purely isometric and eccentric isokinetic contractions at distinct lengths (0.75, 0.8, 0.85, 0.9 and 0.95 L/L_0). n.s. means not significant ($p < 0.05$). n is the number of samples.

	control								
	stress (P/P_0)				paired samples test				
	isometric		eccentric		paired differences				
					95% confidence interval of the difference				
length (L/L_0)	mean	s.d.	mean	s.d.	lower	upper	t	n	p-value (two-tailed)
0.75	0.03	0.03	0.03	0.01	−0.01	0.02	0.51	11	0.62 (n.s.)
0.80	0.08	0.07	0.12	0.02	−0.09	0.01	−1.67	11	0.13 (n.s.)
0.85	0.17	0.10	0.24	0.04	−0.14	0.00	−2.12	11	0.06 (n.s.)
0.90	0.32	0.11	0.42	0.08	−0.21	0.00	−2.18	11	0.05 (n.s.)
0.95	0.61	0.14	0.71	0.14	−0.26	0.06	−1.45	11	0.18 (n.s.)

mediates these phenomena in cardiac muscle. However, the underlying molecular mechanisms, in particular during long eccentric contractions of myocardium, remain(s) unknown [39,40].

Comparing the mechanical response of skeletal [5] and cardiac muscle exposes differences in the underlying microstructure, in the force-producing mechanisms, and in the functioning of the respective muscles. Hence, the aim of our study was to investigate total force generation in intact cardiac trabeculae during extensive isokinetic eccentric contractions in order to examine a potential contribution of a calcium-dependent, adjustable spring element (i.e. titin) to total force. Since potential titin–actin interactions in skeletal muscle [41] will result in enhanced forces after active muscle lengthening, we further aimed to investigate, if RFE exists in cardiac muscle tissue or if it does not.

To achieve these goals, we used a custom-built work-loop calorimeter [42,43] to perform *in vitro* isokinetic ramp experiments on functionally intact cardiac trabeculae obtained from adult rats and stretched the muscle over the whole physiological working range of the FLR. To characterize the contribution of XB and non-XB structures to force production, we used the actin–myosin inhibitor blebbistatin. Findings deduced from such experiments not only improve our understanding of the underlying processes leading to force generation, but also have a significant impact on (multibody) simulation studies of human or animal movement [44].

2. Methods

A total of 11 intact trabeculae from six rat hearts were transferred to the measurement device and mounted between two platinum hooks connected to a custom laser interferometer-based force transducer and a linear length motor [42]. A detailed description of the experimental set-up, handling and preparation of cardiac trabeculae is given in the electronic supplementary material, text S1 and S2. All experiments were conducted in accordance with protocols approved by the University of Auckland Animal Ethics Committee.

(a) Experimental protocol

All experiments were performed at room temperature (22°C). To study the link between force responses and eccentric ramp contractions at constant Ca^{2+} concentrations, stable tetanic contractions were implemented in accordance with a previously established protocol proposed by Pavlov & Landesberg [45]. Fully fused tetanic contraction of the cardiac trabecula was achieved by using a high electrical stimulation frequency (10 Hz) with pulse amplitude of 5 V and pulse width of 5 ms (in the presence of 10 mmol l^{-1} caffeine and an elevated Ca^{2+} concentration of 5 mmol l^{-1} in the 'modified Tyrode solution') [43]. Caffeine was added to induce the release of sarcoplasmic calcium [46] facilitating a tetanic contraction.

To investigate the isometric FLR, each trabecula underwent a series of six to seven isometric contractions. Starting from L_0 (the muscle length associated with the maximally developed isometric force F_0), the length was decreased by increments of 0.05 L_0 up to a minimal muscle length of 0.75 L_0 (cf. figure 1*a*, diamonds). At the minimum length, L_{min}, the active force was negligible. At each length, the force was allowed to reach a steady state, which was typically obtained 40 s after commencing stimulation. The steady state of force was assumed, if the force changed less than 5% over a period of 10 s. To avoid muscle damage induced by excessive lengthening, the trabeculae were not stretched beyond the optimal muscle length [47]. At optimal muscle length, we assumed an SL of 2.2 µm [48]. Beyond this length, the passive force development, which is mainly attributed to a contribution from extracellular structures such as collagen (and intracellular titin), will rise significantly [49–51] (figure 1*a*, grey dotted line).

After finishing the isometric ramp protocol as described above, the trabecula was then subjected to eccentric ramp perturbations comprising two interventions. The first intervention was designed to investigate the dynamic force response during an isokinetic stretch of large magnitude, i.e. from the minimum muscle length to the optimal muscle length in the 'modified Tyrode solution'. The second intervention involved partitioning the non-XB contribution to force development from that of an XB.

During the eccentric ramp perturbation experiment (first intervention), the trabecula was lengthened with and without stimulation from a minimal muscle length of 0.75 L_0 to an

optimal muscle length of 1.0 L_0. All stretches were performed at a velocity of 10% of the maximum shortening velocity, v_{max}: = 2.00 $L_0\,s^{-1}$, which corresponds to 12–14 $\mu m\,s^{-1}$. This is consistent with the maximal unloaded shortening velocity for rat ventricular trabeculae [52,53]. To investigate the individual force responses in cardiac muscle during the steady state, isometric phase post isokinetic ramps (RFE), we continued to apply the stimulation for at least 120 s after the end of the stretch contractions. To calculate RFE, we measured the difference between the redeveloped and the corresponding purely isometric force (prior to the active stretch) at the same length and at 70 and 80 s after the end of each ramp.

The second intervention of the eccentric ramp perturbation experiment was a repeat of the first intervention but in the presence of 15 $\mu mol\,l^{-1}$ blebbistatin dissolved in a polar aprotic solvent—0.4% DMSO in the 'modified Tyrode solution'. This photosensitive chemical is a selective inhibitor of myosin II ATPase that hampers the myosin myofilament from interacting with the actin filament, thereby inhibiting phosphate release and XB-based force development [35]. The blebbistatin concentration does not alter the Ca^{2+} sensitivity of the contractile filaments [54] nor the excitation–contraction coupling [55]. Further, it does not affect titin mobility [35].

To conserve structural, mechanical and functional integrity as well as preventing fatigue of trabeculae, tetani were induced approximately every 40 s during the isometric FLR studies, i.e. between length changes, and about every 80 s between eccentric ramp perturbations. This follows a previously described protocol [45]. For calculating force degradation, isometric reference contractions were performed at L_0 before and after the ramp experiments.

(b) Data processing and statistics

LabVIEW software (National Instruments) was used for data acquisition. For data analysis, a custom-written MATLAB (MathWorks, Nattick, MA, USA) program was used. Data were expressed as mean ± standard deviation (s.d.) unless stated otherwise. For statistically analysing force values, we converted them to stresses (P) with respect to the muscle cross-sectional area (CSA). Unless stated otherwise, they were expressed in absolute values and in kilopascals or normalized to the individual maximal muscle stress (P/P_0). Length values were expressed relative to the optimal muscle length (L/L_0). The two-tailed paired Student's t-test was used to identify significant differences between mean stress values and to compare the calculated individual RFE values to the corresponding isometric reference values prior to the active stretch experiments. A significance level of $p < 0.05$ was used for all analyses. Statistical analyses were realized using SPSS 25 (IBM Corp., Armonk, NY, USA).

3. Results

(a) Stress production in eccentric contractions

Figure 1*a* provides for cardiac trabeculae a direct comparison between the total isokinetic stress–length relation during eccentric stretch (dark blue line) and the steady-state total isometric stress–length relation (black dashed line). For cardiac muscles, both traces show a nonlinear behaviour. Further, they are not statistically different from each other (marked as 'n.s.') when comparing individual stress values at distinct lengths of 0.75 L_0, 0.8 L_0, 0.85 L_0, 0.9 L_0 and 0.95 L_0 (table 1). During eccentric contraction experiments, the isometric stress decreased in successive activations at an average rate of 1.5% per activation.

(b) Isometric stress–length characteristics

The total isometric stress–length relation of cardiac muscle was examined between approximately 1.6 μm and 2.2 μm SL (figure 1*a*, black dashed line). This range closely corresponds to the ascending limb of the stress–length relation of skeletal muscle (cf. figure 1*b*, inset) [2,56]. As demonstrated by previous investigations [2,4,57], the excised rat heart trabeculae featured a monotonically increasing FLR. This is in contrast with the typical slope change between the shallow and steep slope regions at the ascending limb of the FLR in striated skeletal muscles [5,56]. In cardiac muscle, the mean total stress was at 0.75 L_0 about 3% of the maximal isometric stress, P_0, accompanied with zero passive stress (figure 1*a*, grey dotted line). The intercept with the x-axis, where active stress is assumed to be zero, remains at about 0.70 L_0, which corresponds to SLs of about 1.6 μm [1,4]. The mean total stress at the optimal muscle length, $L_0 \approx 2.2$ μm, was 22.98 ± 7.67 kPa, whereas the passive stress was 6.31 ± 3.39 kPa (mean ± s.d.). The proportion of passive stresses with respect to total isometric stresses at L_0 was about 35% P_0 [58]. At physiological muscle lengths from 0.7 L_0 to 1.0 L_0 (corresponding to 1.6–2.2 μm SL [4,59]), the passive stress is in cardiac muscle tissues mainly modulated by titin [35,60]. For muscle lengths larger than 1.0 L_0, e.g. due to acute heart failure [60], passive stiffness predominantly increases due to collagen fibres (pathological stiffness in diseased hearts) [51,60].

(c) Effects of cross-bridge kinetics on eccentric stress generation

Blebbistatin successfully inhibited active isometric muscle stress and leads to marginal levels of XB-based stress production at L_0 (figure 2). A summary of the *in vitro* results of all isokinetic stretch experiments carried out herein is shown in figure 3. For different extensions applied to intact cardiac trabeculae (boundary conditions), the relative total stress response, i.e. the individual trabeculae stresses normalized with respect to the corresponding P_0, were plotted against relative muscle length. The dark blue line in figure 3 reflects the total stress response during the isokinetic stretch (at a rate of 10% v_{max} from 0.75 L_0 to L_0). The light blue line depicts the total stress response under blebbistatin conditions (inhibited XB contribution). The red solid line represents the passive stress–length trace without stimulation. Compared to the control contraction without blebbistatin (figure 3; dark blue line), one can observe a reduction in stress during the eccentric ramp experiment stretching, i.e. from 0.75 to 1.0 L_0 (figure 3; light blue line). The reduced stress obtained through administering blebbistatin was not statistically different from the passive stress (figure 3; red solid line).

(d) Isometric stress development after eccentric isokinetic ramp experiments

Figure 2 shows a representative plot of an eccentric ramp experiment measuring the existence of RFE in cardiac muscle (dark blue solid line). For this case, an intact trabecula was set to a pre-determined muscle length (0.75 L_0) before being activated (at $t = 0$ s). Note that the total muscle stress at length 0.75 L_0 was almost zero (see also figure 1*a*). As

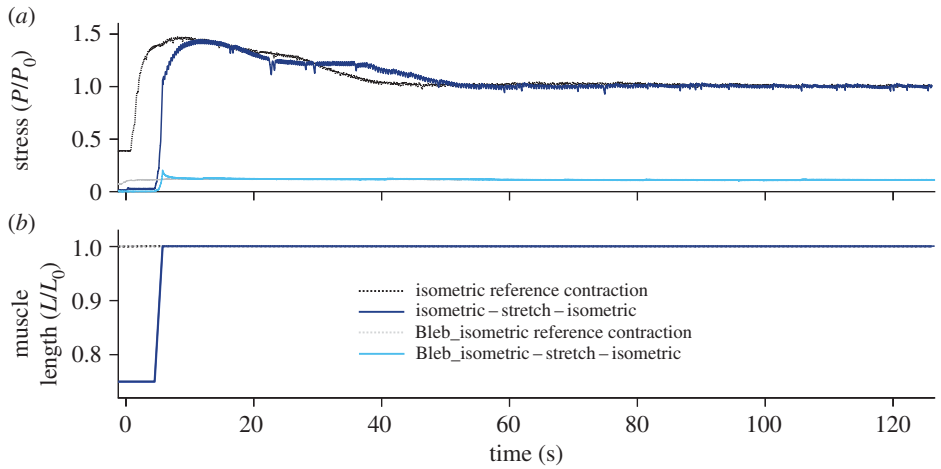

Figure 2. Examination of RFE in cardiac muscle with and without XB inhibition. Raw data of representative normalized stress–time (*a*) and normalized length–time traces (*b*) ($n = 1$) underlying isokinetic length changes with ramp amplitudes of 0.25 L_0 at constant velocity of 10% v_{max}. Notably, with the onset of stimulation at $t = 0$ s, the intact trabecula contracted maximally and produced about 3% active muscle stress (P/P_0) at 0.75 L_0 (dark blue line; table 1). This is in agreement with other studies reporting almost no active muscle force at 0.7 L_0–0.75 L_0 [4,38,57,59]. There is no RFE in intact cardiac trabecula following active stretching under control conditions (dark blue solid line; no XB inhibition (without blebbistatin)) nor under blebbistatin conditions (light blue solid line; with XB inhibition). The black dotted line indicates the isometric reference contraction. The grey dotted line indicates the isometric reference contraction underlying XB inhibition. Note that isometric contractions exhibited an initial, transient force peak (at about 10 s), which is typical for caffeine-induced tetanic contractions of intact heart muscle [43,46,61].

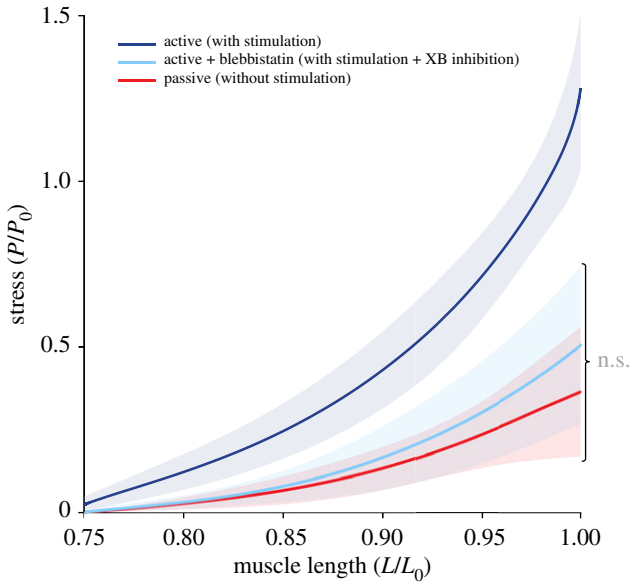

Figure 3. Stress–length relations obtained from isokinetic stretches at different contractile conditions. The mean (solid lines) and s.d. (shaded regions around solid lines) of $n = 11$ cardiac trabeculae undergoing active control (dark blue line) and XB inhibited (using blebbistatin; light blue line) contractions. The red line represents the passive eccentric stress response (in the absence of stimulation). No statistical difference (marked as 'n.s.') between the light blue line and the red line is observed.

the stimuli caused the trabecula to contract, the stretch of the trabecula returned to 1.0 L_0 before isometrically holding it until the maximal steady-state isometric stress was reached. If compared to the isometric reference contraction at L_0, the cardiac trabecula showed virtually no increased stress in the steady-state phase after finishing the ramp perturbation and thus showed no RFE (electronic supplementary material, table T1). After performing the ramp experiments, the stretching of the trabecula was repeated, however, in the presence of 15 µmol l^{-1} blebbistatin. This was done to separate XB and non-XB contributions. After the end of the stretch contraction, the cardiac trabecula showed no RFE (no statistical significance; electronic supplementary material, table T1) during the steady-state phase (figure 2, light blue solid line) if compared to the isometric reference contraction at the same length (figure 2, grey dotted line).

4. Discussion

This study presents the first investigation of the mechanical behaviour of intact cardiac trabeculae during and following extensive isokinetic eccentric ramp contractions. Our experiments reveal two characteristic features: (i) in cardiac muscle and for length values from 0.75 L_0 to 0.95 L_0, there is no significant difference between the eccentric isokinetic stress–length relation and the total isometric stress–length relation. Further, (ii) (residual) FE is not present in cardiac muscle while stretching the muscle from 0.75 to 1.0 optimum muscle length. These results are in strong contrast to those obtained in skeletal muscle during and following extensive stretch contractions (figure 1) [5,16,35]. The underlying experimental findings suggest that there exists in functionally intact, activated cardiac muscle no additional contribution to overall force development by a spring-like element such as titin. These findings stimulate interpretation and speculation. Various studies, which are backed with experimental data, suggest that the mechanical properties of myocardium are affected by the interaction of actin and titin [30,34,36,62] (for recent reviews, see [20,63]). Moreover, these titin(PEVK)–actin interactions might be diminished by the S100A1/Ca^{2+} complex [32,64], where S100A1 is a soluble calcium-binding protein. Based on this ample evidence, it can be hypothesized that the underlying observations can be deduced from an inverse relationship of titin–actin binding that occurs upon muscle activation by S100A1/Ca^{2+}. Consequently, the results of the present study support the following assumptions: (i) upon cardiac muscle activation, potential changes in stiffness of single titin molecules result

only in a negligible titin-related effect and (ii) the diminishing or the release of titin–actin interactions in cardiac muscle is a function of increasing Ca^{2+} concentrations and, thus, no or negligible increase in titin-based stiffness and force during active eccentric ramp contractions can be observed.

Despite these speculations, the experimental observations presented in this study reveal that cardiac muscle has, in its intact form, a force-producing mechanism that is distinct from that of skeletal muscle. This mechanism exhibits largely enhanced forces during extensive lengthening contractions [5] and substantial RFE [11,14,65]—effects that are well acknowledged and a main determinant of active force production of skeletal muscle [13,20].

(a) Comparison with skeletal muscle

(i) Structural properties of titin

The differences in contractile behaviour observed between cardiac and skeletal musculature could be attributed to their functional and morphological variations. One variation may reside in the (I-band) structure of the sarcomeric, filamentous spring protein titin, which spans half a sarcomere from the Z-disc to the M-line. Titin firmly anchors to myosin in the A-band region and then runs freely across the I-band region of the sarcomere until it attaches to actin (approx. 50–100 nm away from the Z-band) before finally entering the Z-band. Thereby, it forms a 'permanent' bridge between actin and myosin [66]. In skeletal muscle, the I-band titin consists of a proximal and distal immunoglobulin domain, a PEVK region (abundant in the amino acids proline (P), glutamate (E), valine (V) and lysine (K)) and an N2A region [67]. Cardiac titin is known to express two isoforms, namely an N2B isoform, which predominantly exists in small mammals such as rat and rabbit, and an N2BA isoform, which occurs in large mammals such as bovines. The N2B isoform is much shorter than the N2BA or the N2A isoform [68]. Through alternative splicing of the I-band titin, cardiac and skeletal muscles express titin springs with varying lengths (primarily of the PEVK domain), which correlate with the passive properties of different muscle types [63,66,69]. In addition, the ratio of N2BA/N2B expression varies in heart tissue between the atria and ventricles and has been attributed to various heart diseases [60,63]. Moreover, if compared to skeletal muscle titin, titin within heart tissue has short IG and PEVK segments exhibiting less E-rich domains [63,70,71]. In addition to these structural differences, skeletal muscles are more prone to show an increase in titin-induced force during and after stretch contractions than cardiac muscle [35,36] (cf. §4*a*(ii)). Differences in the isometric stress–length relation between cardiac and skeletal muscle were discussed in electronic supplementary material, text S3.

(ii) Potential titin contribution to total force development during stretch

The observed nonlinear stress behaviour of intact cardiac trabeculae during extensive muscle lengthening contractions (figure 1*a*, blue solid line) is in contrast with the linear stress behaviour in skeletal muscles during comparable lengthening experiments, e.g. in single myofibres (cf. figure 1*b*; [5]) or whole muscle preparations [72]. Specifically, experimental observations on striated skeletal muscle tissue demonstrated that single muscle fibres taken from the rat EDL muscle have a linear spring-like behaviour during long eccentric contractions (nearly over the entire physiological FLR; cf. figure 1*b*, inset). Within this work, we also demonstrated that both XBs and non-XBs nonlinearly contribute to the resulting linear total muscle stress response. Active isokinetic stretching of permeabilized skeletal muscle fibres from 0.75 L_0 to 1.0 L_0 revealed an increase in stress by about 60% (figure 1*b*). This clearly exceeds the maximum active stresses produced by XBs at these lengths. Statistical analyses yielded highly significant differences between eccentric and isometric stress–length traces under active conditions (pCa 4.5) in permeabilized muscle fibres (cf. figure 1*b*; [5]). Explanatory approaches [22,24,25], in which titin plays a crucial role in contributing to the progressive force response during active stretch contractions, seem to overcome significant deviations between experimental observations in skeletal muscle [5,11] and predictions from the sliding filament and XB theories.

In skeletal muscles, two of the main concepts by which titin might contribute to increased forces during and following stretches are: (i) the stiffening of the single titin molecules due to muscle activation [70] and (ii) the reduction in the titin's free spring length due to titin–actin interactions [24]. Further, titin–actin binding seems possible in skeletal muscle when calcium is present [41]. In skeletal muscle, such attachments may occur between myosin binding sites of the actin filament [27,73] and the titin's PEVK [28,29] or N2A [74] region (or with some other structure within the sarcomere). However, the impact of Ca^{2+} on titin–actin binding appears to be inconclusive and thus requires further examination by a systematic re-evaluation of existing findings under different boundary conditions, especially considering structural and biochemical differences between different muscle types (skeletal, heart, smooth muscles).

(iii) Chemical cross-bridge inhibition during stretch

Numerous experimental investigations on skeletal muscle observed enhanced forces during eccentric contractions [5,65]. There are several hints that these enhanced forces are due to increased non-XB forces. A series of experiments, in which XB formation is hampered by actomyosin inhibitors, enabled the estimation of non-XB contributions to FE. Labeit *et al*. [70] observed increased (approx. 20%) non-XB-based (titin) forces in activated permeabilized mice muscle fibres (pCa 4.0, XBs inhibited by the use of 2,3-butanedione monoxime (BDM)) compared to passively (pCa 9.0) stretched myofibres. These results have been confirmed by other studies using blebbistatin [35,36]. Furthermore, by performing active stretch experiments at very long SLs (no actin–myosin overlap; thereby excluding XB formation), Leonard & Herzog [16] measured higher forces than during passive stretches, indicating the presence of titin-based forces. Thus, these studies suggest an additional contribution of non-XB-based forces (titin) to total force during and after active stretch in skeletal muscle. This is in contrast with the behaviour of cardiac trabeculae during eccentric contractions showing no difference between active force production when XBs are inhibited and purely isokinetic passive stretching (figure 3, compare light blue with red line). A possible explanation for the differences between cardiac and skeletal muscles might be the property of cardiac (PEVK-) titin–

actin binding diminishing with increasing Ca^{2+}, thereby decreasing titin-based stiffness and force [30–32,63].

5. Conclusion

The presented results for intact trabeculae are consistent with the results of studies that investigate RFE in cardiac myofibril with permeabilized preparations [35,36]. In [35], homogenization of pieces of papillary muscle yielded isolated myofibrils that were activated by increasing Ca^{2+} concentrations within the solutions. The focus of [35] was on investigating the steady-state force response of permeabilized cardiac myofibrils after isokinetic eccentric muscle contractions (10 $\mu m\ s^{-1}$) with different stretch magnitudes (SLs ranging from 1.80 to 2.29 μm). The results of both studies [35,36] confirm that RFE is not present in the heart—neither in control conditions (figure 2, compare dark blue line with black dashed line) nor during XB inhibition (figure 2, compare light blue line with grey dashed line). Anyhow, we performed active stretch experiments in an extensive length range (0.75 L_0–1.0 L_0) and there is no systematic study investigating the effect of varying stretch amplitudes and starting lengths on (residual-) FE in intact cardiac preparations. Hence, since the stretch amplitude is believed to be an important parameter for improving our understanding of the underlying mechanism(s) of (R)FE [10], different initial lengths and degrees of stretch should be considered in future studies that aim to examine the effect of titin on force responses in myocardial tissue. Notably, the current finding in cardiac muscle is in sharp contrast to previous results in skeletal muscle [11,12,14,36] (see electronic supplementary material, text S4, for further information of the functional relevance of FE).

Moreover, both approaches (of the current study and those of [35,36]) indirectly support the claim that the increase in force upon muscle activation and stretching of skeletal muscle is directly associated with titin isoforms [20]. Conversely, the data of this study support the hypothesis that titin stiffness does not increase with activation in intact cardiac muscle. This conclusion is backed by ample evidence, suggesting that titin–actin interaction in cardiac tissue decreases with increasing concentrations of calcium [30,31] or remains unaffected [32,34,62]. This finding is in contrast with observations in skeletal muscle [41].

Differences in titin structure and titin–actin behaviour between cardiac and skeletal muscle might be responsible for the observed deviations in active eccentric contractions (figure 1). Due to the lack of RFE and the absence of increased non-XB-based stiffness and forces in cardiac muscle during active stretch (from 0.75 L_0 to 1.0 L_0), our findings indirectly support the theory that there is an inverse effect of an adjustable titin spring contributing to titin-based stiffness in cardiac muscles [24]. However, mechanical properties of titin continually adapt to cover prevailing conditions of cardiac contractile performance. This adaptation (in particular phosphorylation-mediated regulation) is complex and can be modulated by various protein kinases [75,76]. The modulation depends on the location where protein kinase phosphorylates the elastic titin regions [76]. For instance, phosphorylation of the cardiac N2B region increases the persistence length of the elastic titin spring, which results in reduced overall titin-based stiffness and force. By contrast, phosphorylation of the PEVK region reduces the effective free spring length yielding increased stretch-dependent stiffness and force [76]. Hence, it is expected that titin makes a complex contribution to several phases of the cardiac cycle. Titin stiffness is closely related to ventricular function, whereas titin compliance has been shown to improve diastolic function [60]. The present findings underline the physiological relevance and the beneficial effect of titin on maintaining global cardiac functionality, e.g. as a function of physical activity [77].

The observations of this study add another aspect to the overwhelming published evidence, suggesting that decreased titin stiffness causes reduced length-dependent activation (LDA). LDA is an integral part and the cellular basis of the Frank–Starling mechanism, responsible for the elevated cardiac output in response to increased preload [77].

In summary, our data support, although indirectly, several hypotheses based on experimental findings which suggest that during the cardiac cycle, the interaction between titin and actin varies. It has been shown that this interaction can be modulated by S100A1, a soluble calcium-binding protein found at high concentrations in the myocardium [20]. Hence, titin–actin interaction seems to be strong during diastolic filling when the level of the Ca^{2+}/S100A1 complex is low, but considerably weaker during systole when Ca^{2+}/S100A1 is high [30–32,34].

Data accessibility. All necessary data and information are provided in the electronic supplementary material so that published research is fully reproducible and the results reported can be verified.

Authors' contributions. A.T., O.R. and T.S. conceived and developed the ideas. A.T. and T.S. designed the experiments. A.T., T.P. and J.-C.H. performed the measurements. A.J.T. developed, constructed and built the experimental set-up and supervised the experimental data acquisition. A.T. analysed the data, prepared the figures, performed the statistical analyses and drafted the first version of the manuscript. T.S., O.R., J.-C.H. and A.J.T. assisted by drafting the final version of the manuscript. All authors gave final approval for publication.

Competing interests. We have no competing interests.

Funding. This work was supported by the Deutsche Forschungsgemeinschaft (DFG) under grants SI841/15-1 and SI841/17-1 as well as part of the International Graduate Research Group on Soft Tissue Robotics—Simulation-Driven Concepts and Design for Control and Automation for Robotic Devices Interacting with Soft Tissues (GRK 2198/1).

Acknowledgements. The authors would like to thank Dr Kenneth Tran for stimulating discussions on data interpretation. We acknowledge funding of Marsden Fast-start grants from the Royal Society of New Zealand (UOA1504) and an Emerging Researcher First Grant from the Health Research Council of New Zealand (16/510).

References

1. Allen D, Jewell B, Murray J. 1974 The contribution of activation processes to the length–tension relation of cardiac muscle. *Nature* **248**, 606–607. (doi:10.1038/248606a0)

2. Rassier DE. 2000 The degree of activation of cardiac muscle depends on muscle length. *Arq. Bras.*

Cardiol. **75**, 454–457. (doi:10.1590/S0066-782X2000001100009)

3. Ter Keurs HEDJ, Rijnsburger WH, Van Heuningen R, Nagelsmit MJ. 1980 Tension development and sarcomere length in rat cardiac trabeculae. Evidence of length-dependent activation. *Circ. Res.* **46**, 703–714. (doi:10.1161/01.RES.46.5.703)
4. Huntsman LL, Rondinone JF, Martyn DA. 1983 Force–length relations in cardiac muscle segments. *Am J Physiol* **244**, H701–H707. (doi:10.1152/ajpheart.1983.244.5.h701)
5. Tomalka A, Rode C, Schumacher J, Siebert T. 2017 The active force–length relationship is invisible during extensive eccentric contractions in skinned skeletal muscle fibres. *Proc. R. Soc. B* **284**, pii: 20162497. (doi:10.1098/rspb.2016.2497)
6. Winters TM, Takahashi M, Lieber RL, Ward SR. 2011 Whole muscle length–tension relationships are accurately modeled as scaled sarcomeres in rabbit hindlimb muscles. *J. Biomech.* **44**, 109–115. (doi:10.1016/j.jbiomech.2010.08.033)
7. Burkholder TJ, Lieber RL. 2001 Sarcomere length operating range of vertebrate muscles during movement. *J. Exp. Biol.* **204**, 1529–1536.
8. Mörl F, Siebert T, Häufle D. 2016 Contraction dynamics and function of the muscle–tendon complex depend on the muscle fibre–tendon length ratio: a simulation study. *Biomech. Model. Mechanobiol.* **15**, 245–258. (doi:10.1007/s10237-015-0688-7)
9. Biewener AA. 1998 Muscle function *in vivo*: a comparison of muscles used for elastic energy savings versus muscles used to generate mechanical power. *Am. Zool.* **38**, 703–717. (doi:10.1093/icb/38.4.703)
10. Abbott BC, Aubert XM. 1952 The force exerted by active striated muscle during and after change of length. *J. Physiol.* **117**, 77–86. (doi:10.1113/jphysiol.1952.sp004733)
11. Leonard TR, DuVall M, Herzog W. 2010 Force enhancement following stretch in a single sarcomere. *Am. J. Physiol.-Cell Physiol.* **299**, C1398–C1401. (doi:10.1152/ajpcell.00222.2010)
12. Joumaa V, Leonard TR, Herzog W. 2008 Residual force enhancement in myofibrils and sarcomeres. *Proc. R. Soc. B* **275**, 1411–1419. (doi:10.1098/rspb.2008.0142)
13. Edman KAP, Elzinga G, Noble M. 1982 Residual force enhancement after stretch of contracting frog single muscle fibers. *J. Gen. Physiol.* **80**, 769–784. (doi:10.1085/jgp.80.5.769)
14. Siebert T, Leichsenring K, Rode C, Wick C, Stutzig N, Schubert H, Blickhan R, Böl M. 2015 Three-dimensional muscle architecture and comprehensive dynamic properties of rabbit gastrocnemius, plantaris and soleus: input for simulation studies. *PLoS ONE* **10**, e0130985. (doi:10.1371/journal.pone.0130985)
15. Hahn D, Seiberl W, Schmidt S, Schweizer K, Schwirtz A. 2010 Evidence of residual force enhancement for multi-joint leg extension. *J. Biomech.* **43**, 1503–1508. (doi:10.1016/j.jbiomech.2010.01.041)
16. Leonard TR, Herzog W. 2010 Regulation of muscle force in the absence of actin–myosin-based cross-bridge interaction. *Am. J. Physiol. Cell Physiol.* **299**, C14–C20. (doi:10.1152/ajpcell.00049.2010)
17. Campbell SG, Campbell KS. 2011 Mechanisms of residual force enhancement in skeletal muscle: insights from experiments and mathematical models. *Biophys. Rev.* **3**, 199–207. (doi:10.1007/s12551-011-0059-2)
18. Edman KAP. 2010 Contractile performance of striated muscle. *Adv. Exp. Med. Biol.* **682**, 7–40. (doi:10.1007/978-1-4419-6366-6_2)
19. Hiepe P, Herrmann KH, Güllmar D, Ros C, Siebert T, Blickhan R, Hahn K, Reichenbach JR. 2014 Fast low-angle shot diffusion tensor imaging with stimulated echo encoding in the muscle of rabbit shank. *NMR Biomed.* **27**, 146–157. (doi:10.1002/nbm.3046)
20. Rassier DE. 2017 Sarcomere mechanics in striated muscles: from molecules to sarcomeres to cells. *Am. J. Physiol. - Cell Physiol.* **313**, C134–C145. (doi:10.1152/ajpcell.00050.2017)
21. Wang K, McClure J, Tu A. 1979 Titin: major myofibrillar components of striated muscle. *Proc. Natl Acad. Sci. USA* **76**, 3698–3702. (doi:10.1073/pnas.76.8.3698)
22. Nishikawa KC, Monroy JA, Uyeno TE, Yeo SH, Pai DK, Lindstedt SL. 2012 Is titin a 'winding filament'? A new twist on muscle contraction. *Proc. R. Soc. B* **279**, 981–990. (doi:10.1098/rspb.2011.1304)
23. Schappacher-Tilp G, Leonard T, Desch G, Herzog W. 2015 A novel three-filament model of force generation in eccentric contraction of skeletal muscles. *PLoS ONE* **10**, e0117634. (doi:10.1371/journal.pone.0117634)
24. Rode C, Siebert T, Blickhan R. 2009 Titin-induced force enhancement and force depression: a 'sticky-spring' mechanism in muscle contractions? *J. Theor. Biol.* **259**, 350–360. (doi:10.1016/j.jtbi.2009.03.015)
25. Heidlauf T, Klotz T, Rode C, Siebert T, Röhrle O. 2017 A continuum-mechanical skeletal muscle model including actin–titin interaction predicts stable contractions on the descending limb of the force-length relation. *PLoS Comput. Biol.* **13**, 1–25. (doi:10.1371/journal.pcbi.1005773)
26. Till O, Siebert T, Blickhan R. 2010 A mechanism accounting for independence on starting length of tension increase in ramp stretches of active skeletal muscle at short half-sarcomere lengths. *J. Theor. Biol.* **266**, 117–123. (doi:10.1016/j.jtbi.2010.06.021)
27. Astier C, Raynaud F, Lebart MC, Roustan C, Benyamin Y. 1998 Binding of a native titin fragment to actin is regulated by PIP2. *FEBS Lett.* **429**, 95–98. (doi:10.1016/S0014-5793(98)00572-9)
28. Bianco P, Nagy A, Kengyel A, Szatmári D, Mártonfalvi Z, Huber T, Kellermayer MSZ. 2007 Interaction forces between F-actin and titin PEVK domain measured with optical tweezers. *Biophys. J.* **93**, 2102–2109. (doi:10.1529/biophysj.107.106153)
29. Nagy A. 2004 Differential actin binding along the PEVK domain of skeletal muscle titin. *J. Cell Sci.* **117**, 5781–5789. (doi:10.1242/jcs.01501)
30. Kulke M, Fujita-Becker S, Rostkova E, Neagoe C, Labeit D, Manstein DJ, Gautel M, Linke WA. 2001 Interaction between PEVK-titin and actin filaments: origin of a viscous force component in cardiac myofibrils. *Circ. Res.* **89**, 874–881. (doi:10.1161/hh2201.099453)
31. Linke WA, Kulke M, Li H, Fujita-becker S, Neagoe C, Manstein DJ, Gautel M, Fernandez JM. 2002 PEVK domain of titin: an entropic spring with actin-binding properties. *J. Struct. Biol.* **205**, 194–205. (doi:10.1006/jsbi.2002.4468)
32. Yamasaki R *et al.* 2001 Titin–actin interaction in mouse myocardium: passive tension modulation and its regulation by calcium/S100A1. *Biophys. J.* **81**, 2297–2313. (doi:10.1016/S0006-3495(01)75876-6)
33. Trombitas K, Granzier H. 1997 Actin removal from cardiac myocytes shows that near Z line titin attaches to actin while under tension. *Am. J. Physiol.* **273**, C662–C670. (doi:10.1152/ajpcell.1997.273.2.C662)
34. Fukushima H, Chung CS, Granzier H. 2010 Titin-isoform dependence of titin–actin interaction and its regulation by S100A1/Ca^{2+} in skinned myocardium. *J. Biomed. Biotechnol.* **2010**, 727239. (doi:10.1155/2010/727239)
35. Shalabi N, Cornachione A, Leite F, Vengallatore S, Rassier DE. 2017 Residual force enhancement is regulated by titin in skeletal and cardiac myofibrils. *J. Physiol.* **595**, 2085–2098. (doi:10.1113/JP272983)
36. Cornachione AS, Leite FS, Bagni MA, Rassier DE. 2016 The increase in non-crossbridge forces after stretch of activated striated muscle is related to titin isoforms. *Am. J. Physiol. Cell Physiol.* **310**, C19–C26. (doi:10.1152/ajpcell.00156.2015)
37. Patterson SW, Piper H, Starling EH. 1914 The regulation of the heart beat. *J. Physiol.* **48**, 465–513. (doi:10.1113/jphysiol.1914.sp001676)
38. Allen DG, Kurihara S. 1982 The effects of muscle length on intracellular calcium. *J. Physiol.* **327**, 79–94. (doi:10.1113/jphysiol.1982.sp014221)
39. Ait-Mou Y, Zhang M, Martin JL, Greaser ML, de Tombe PP. 2017 Impact of titin strain on the cardiac slow force response. *Prog. Biophys. Mol. Biol.* **130**, 281–287. (doi:10.1016/j.pbiomolbio.2017.06.009)
40. Sequeira V, van der Velden J. 2017 The Frank–Starling Law: a jigsaw of titin proportions. *Biophys. Rev.* **9**, 259–267. (doi:10.1007/s12551-017-0272-8)
41. Kellermayer M, Granzier HL. 1996 Calcium-dependent inhibition of *in vitro* thin-filament motility by native titin. *FEBS Lett.* **380**, 281–286. (doi:10.1016/0014-5793(96)00055-5)
42. Taberner AJ, Han J-C, Loiselle DS, Nielsen PMF. 2011 An innovative work-loop calorimeter for *in vitro* measurement of the mechanics and energetics of working cardiac trabeculae. *J. Appl. Physiol.* **111**, 1798–1803. (doi:10.1152/japplphysiol.00752.2011)
43. Han J, Taberner AJ, Kirton RS, Nielsen PM, Smith NP, Loiselle DS. 2009 A unique micromechanocalorimeter for simultaneous measurement of heat rate and force production of

cardiac trabeculae carneae. *J. Appl. Physiol.* **107**, 946–951. (doi:10.1152/japplphysiol.00549.2009.)

44. Röhrle O, Saini H, Ackland DC. 2017 Occlusal loading during biting from an experimental and simulation point of view. *Dent. Mater.* **34**, 58–68. (doi:10.1016/j.dental.2017.09.005)
45. Pavlov D, Landesberg A. 2016 The cross-bridge dynamics is determined by two length-independent kinetics: Implications on muscle economy and Frank–Starling Law. *J. Mol. Cell. Cardiol.* **90**, 94–101. (doi:10.1016/j.yjmcc.2015.11.007)
46. Gibbs C, Loiselle D. 1978 The energy output of tetanized cardiac muscle: species differences. *Pflügers Arch. Eur. J. Physiol.* **373**, 31–38. (doi:10.1007/BF00581146)
47. Iwazumi T. 1987 Mechanics of the myofibril. In *Mechanics of the Circulation. Developments in Cardiovascular Medicine*, vol. 69 (eds HEDJ Ter Keurs, JV Tyberg). Dordrecht, The Netherlands: Springer. (doi:10.1007/978-94-009-3311-8_3)
48. ter Keurs HE, Luff AR, Luff SE. 1984 Force–sarcomere-length relation and filament length in rat extensor digitorum muscle. *Adv. Exp. Med. Biol.* **170**, 511–525. (doi:10.1007/978-1-4684-4703-3_44)
49. de Tombe P, ter Keurs H. 1990 Force and velocity of sarcomere shortening in trabeculae from rat heart. Effects of temperature. *Circ. Res.* **66**, 1239–1254. (doi:10.1161/01.RES.66.5.1239)
50. Linke WA, Popov VI, Pollack GH. 1994 Passive and active tension in single cardiac myofibrils. *Biophys. J.* **67**, 782–792. (doi:10.1016/S0006-3495(94)80538-7)
51. Linke WA, Fernandez JM. 2002 Cardiac titin: molecular basis of elasticity and cellular contribution to elastic and viscous stiffness components in myocardium. *J. Muscle Res. Cell Motil.* **23**, 483–497. (doi:10.1023/A:1023462507254)
52. Daniels M, Noble MI, ter Keurs HE, Wohlfart B. 1984 Velocity of sarcomere shortening in rat cardiac muscle: relationship to force, sarcomere length, calcium and time. *J. Physiol.* **355**, 367–381. (doi:10.1113/jphysiol.1984.sp015424)
53. de Tombe PP, ter Keurs HE. 2012 The velocity of cardiac sarcomere shortening; mechanisms and implications. *J. Muscle Res. Cell Motil.* **33**, 431–437. (doi:10.1007/s10974-012-9310-0)
54. Dou Y, Arlock P, Arner A. 2007 Blebbistatin specifically inhibits actin–myosin interaction in mouse cardiac muscle. *AJP Cell Physiol.* **293**, C1148–C1153. (doi:10.1152/ajpcell.00551.2006)
55. Farman GP, Tachampa K, Mateja R, Cazorla O, Lacampagne A, De Tombe PP. 2008 Blebbistatin: use as inhibitor of muscle contraction. *Pflugers Arch. Eur. J. Physiol.* **455**, 995–1005. (doi:10.1007/s00424-007-0375-3)
56. Gordon AM, Huxley AF, Julian FJ. 1966 The variation in isometric tension with sarcomere length in vertebrate muscle fibres. *J. Physiol.* **184**, 170–192. (doi:10.1113/jphysiol.1966.sp007909)
57. Allen DG, Kentish JC. 1985 The cellular basis of the length–tension relation in cardiac muscle. *J. Mol. Cell. Cardiol.* **17**, 821–840. (doi:10.1016/S0022-2828(85)80097-3)
58. Julian FJ, Sollins MR. 1975 Sarcomere length tension relations in living rat papillary muscle. *Circ. Res.* **37**, 299–308. (doi:10.1161/01.RES.37.3.299)
59. Kentish J, ter Keurs HE, Ricciardi L, Bucx J, Noble M. 1986 Comparison between the sarcomere length–force relations of intact and skinned trabeculae from rat right ventricle. *Circ. Res.* **58**, 755–768. (doi:10.1161/01.RES.58.6.755)
60. Linke WA, Hamdani N. 2014 Gigantic business: titin properties and function through thick and thin. *Circ. Res.* **114**, 1052–1068. (doi:10.1161/CIRCRESAHA.114.301286)
61. Chapman RA, Miller DJ. 1974 The effects of caffeine on the contraction of the frog heart. *J. Physiol.* **242**, 589–613. (doi:10.1113/jphysiol.1974.sp010725)
62. Linke WA, Ivemeyer M, Labeit S, Hinssen H, Rüegg JC, Gautel M. 1997 Actin–titin interaction in cardiac myofibrils: probing a physiological role. *Biophys. J.* **73**, 905–919. (doi:10.1016/S0006-3495(97)78123-2)
63. Linke WA. 2017 Titin gene and protein functions in passive and active muscle. *Annu. Rev. Physiol.* **80**, 389–411. (doi:10.1146/annurev-physiol-021317-121234)
64. Chung C, Methawasin M, Nelson O, Radke M, Hidalgo C, Gotthardt M, Granzier H. 2011 Titin based viscosity in ventricular physiology: an integrative investigation of PEVK–actin interactions. *J. Mol. Cell. Cardiol.* **51**, 428–434. (doi:10.1016/j.yjmcc.2011.06.006)
65. Abbott B, Bigland B, Ritchie J. 1952 The physiological cost of negative work. *J. Physiol.* **117**, 380–390. (doi:10.1113/jphysiol.1952.sp004755)
66. Prado LG, Makarenko I, Andresen C, Krüger M, Opitz CA, Linke WA. 2005 Isoform diversity of giant proteins in relation to passive and active contractile properties of rabbit skeletal muscles. *J. Gen. Physiol.* **126**, 461–480. (doi:10.1085/jgp.200509364)
67. Labeit S, Kolmerer B. 1995 Titins: giant proteins in charge of muscle ultrastructure and elasticity. *Science* **270**, 293–296. (doi:10.1126/science.270.5234.293)
68. Bang M-L *et al*. 2001 The complete gene sequence of titin, expression of an unusual 700-kDa titin isoform, and its interaction with obscurin identify a novel Z-line to I-band linking system. *Circ. Res.* **89**, 1065–1072. (doi:10.1161/hh2301.100981)
69. Freiburg A *et al*. 2000 Series of exon-skipping events in the elastic spring region of titin as the structural basis for myofibrillar elastic diversity. *Circ. Res.* **86**, 1114–1121. (doi:10.1161/01.res.86.11.1114)
70. Labeit D, Watanabe K, Witt C, Fujita H, Wu Y, Lahmers S, Funck T, Labeit S, Granzier HL. 2003 Calcium-dependent molecular spring elements in the giant protein titin. *Proc. Natl Acad. Sci. USA* **100**, 13 716–13 721. (doi:10.1073/pnas.2235652100)
71. Krüger M, Kötter S. 2016 Titin, a central mediator for hypertrophic signaling, exercise-induced mechanosignaling and skeletal muscle remodeling. *Front. Physiol.* **7**, 1–8. (doi:10.3389/fphys.2016.00076)
72. Till O, Siebert T, Rode C, Blickhan R. 2008 Characterization of isovelocity extension of activated muscle: a Hill-type model for eccentric contractions and a method for parameter determination. *J. Theor. Biol.* **255**, 176–187. (doi:10.1016/j.jtbi.2008.08.009)
73. Niederlader N, Raynaud F, Astier C, Chaussepied P. 2004 Regulation of the actin–myosin interaction by titin. *Eur. J. Biochem.* **271**, 4572–4581. (doi:10.1111/j.1432-1033.2004.04429.x)
74. Dutta S, Tsiros C, Sundar SL, Athar H, Moore J, Nelson B, Gage MJ, Nishikawa K. 2018 Calcium increases titin N2A binding to F-actin and regulated thin filaments. *Sci. Rep.* **8**, 1–11. (doi:10.1038/s41598-018-32952-8)
75. Krüger M, Kötter S, Grützner A, Lang P, Andresen C, Redfield MM, Butt E, Dos Remedios CG, Linke WA. 2009 Protein kinase G modulates human myocardial passive stiffness by phosphorylation of the titin springs. *Circ. Res.* **104**, 87–94. (doi:10.1161/CIRCRESAHA.108.184408)
76. Hamdani N, Herwig M, Linke WA. 2017 Tampering with springs: phosphorylation of titin affecting the mechanical function of cardiomyocytes. *Biophys. Rev.* **9**, 225–237. (doi:10.1007/s12551-017-0263-9)
77. Methawasin M, Hutchinson K, Lee E, Smith J, Saripalli C, Hidalgo C, Ottenheijm C, Granzier H. 2014 Experimentally increasing titin compliance in a novel mouse model attenuates the Frank–Starling mechanism but has a beneficial effect on diastole. *Circulation* **129**, 1924–1936. (doi:10.1161/CIRCULATIONAHA)